

SENSITIVITY ANALYSIS OF WAG 4 GROUNDWATER MODELING

INTRODUCTION

This sensitivity analysis was prepared for the WAG 4 Remedial Investigation/Feasibility Study groundwater pathway. The pathway concentrations were determined using the screening code GWSCREEN, a semi-analytical model that provides groundwater concentrations at receptor locations for use in risk assessment. The concentrations this code simulates provide input for the upper bound of the risk posed through the groundwater pathway.

The original modeling for the WAG 4 RI/FS, which is reported in Section 6 of that report, was based on parameter values which are either accepted INEEL Track 2 default values or where determined from site-specific data. The original modeling results serve as the base case in this sensitivity analysis.

This analysis explores the sensitivity of predicted groundwater concentrations to changes in several modeling parameters. These include changes in the magnitude of the GWSCREEN parameter "depth" which refers to the total thickness of the unsaturated zone. Also analyzed are the effects of changing the direction of groundwater flow beneath WAG 4. Finally, the results of two different versions of the GWSCREEN code, version 2.4a and the user-interface GWMENU, were compared to ensure the use of GWMENU did not produce results different from the well-documented version 2.4a.

MODEL DESCRIPTION

GMENU is a menu-driven user-interface that employs the solution algorithm of GWSCREEN version 2.4a. The advantage of this enhancement is the capability to overlaying an arbitrary grid frame on the entire WAG 4. This grid provides a coordinate system that gives a common reference point to each contaminant source. A receptor network can be included in the grid usually downgradient from the sites, with respect to the groundwater flow direction. The results of individual site simulations can then be compiled with those of other sites containing contaminants in common. A cumulative impact at the receptor network can then be calculated for each contaminant species by superimposing the individual site contributions. This simulates the effect of intermingling groundwater plumes that originate at different contaminated sites but intermingle in the groundwater before reaching a receptor.

The grid framework for the WAG 4 groundwater pathway modeling is based on the location of the most-downgradient, with respect to groundwater flow, contamination source. That site is CFA-04 and is assumed to be the origin of the arbitrary coordinate system. Other sites and the receptor network are referenced to the center of CFA-04. A set of relative "offset" coordinates is provided for each site and each receptor based on the differences between the site or receptor Universal Transverse Meridian (Northing and Easting) coordinates and the coordinates of CFA-04. These relative coordinates are provided in Table x1 along with other site and receptor information.

As described in Section 6 of the WAG 4 Remedial Investigation Baseline Risk Assessment, the modeled sites were assumed to have rectangular horizontal-plane shapes and uniform vertical thicknesses. All of the modeled WAG 4 sites are surface or buried sites; none are modeled as ponds or injection wells. This allows easy reconfiguration of the actual site shapes and dimensions into uniformly-thick right rectangles with dimensions that provide the same contaminated areas and volumes as determined in the Nature and Extent of Contamination section of the WAG 4 RI/BRA. The original WAG 4 RI/BRA groundwater pathway modeling and this subsequent sensitivity analysis includes 14 retained sites and 21 petroleum tanks. Due to the irregularity of their actual shapes, four of the retained sites were divided into two portions each. One of these (CFA-17) is part of a set of two retained sites and one tank that are all located north of TRA but are included in the WAG 4 RI/BRA.

Table x1. Modeling details for each site.

Site	UTM ¹ (East, m)	UTM (North, m)	Offset ² parallel to flow (m)	Offset perpendicular to flow (m)	CVZIT ² (m)	Length (parallel to flow) (m)	Width (perpendicular to flow) (m)	Thickness of source (m)	Area (m ²)	Volume (m ³)	Contaminated Soil Mass (kg)
CFA-13	342910.0	4821062.0	-577.3	174.9	14.0	5.0	5.0	9.1	25.0	227.5	3.41E+05
CFA-15	342759.7	4820694.4	-209.7	24.5	13.5	0.5	0.5	7.9	0.3	2.3	3.46E+03
CFA-04	342735.2	4820484.7	0.0	0.0	14.0	150.7	45.6	5.5	6875.3	37813.2	5.67E+07
CFA-17a	343402.6	4828685.0	-8200.2	667.4	18.5	48.6	33.5	3.8	1629.9	6217.1	9.33E+06
CFA-17b	343390.0	4828718.5	-8233.7	654.9	18.5	18.3	18.1	3.8	331.1	1262.9	1.89E+06
CFA-47	343443.6	4828685.0	-8200.2	708.4	18.5	1.0	1.0	3.8	0.9	3.5	5.27E+03
CFA-07a	343547.3	4821934.0	-1449.2	812.1	46.3	2.7	2.7	3.5	7.3	25.5	3.83E+04
CFA-07b	343550.0	4821936.7	-1451.9	814.8	46.3	2.7	2.7	3.5	7.3	25.5	3.83E+04
CFA-12	342728.6	4821453.5	-968.7	-6.5	12.9	3.7	3.7	2.6	13.4	34.8	5.22E+04
CFA-08	343737.4	4821772.8	-1288.0	1002.2	47.0	305.0	61.0	9.9	18605.0	184189.5	2.76E+08
CFA-08b	344019.3	4822252.9	-1768.1	1284.1	49.0	62.4	89.2	7.6	5566.1	42302.2	6.35E+07
CFA-10	343182.5	4820914.5	-429.8	447.4	19.0	40.7	19.9	3.0	808.1	2463.1	3.69E+06
CFA-26	342821.6	4820851.5	-366.7	86.4	13.0	30.5	30.5	5.0	930.3	4651.3	6.98E+06
CFA-42	343695.9	4821661.0	-1176.2	960.7	40.9	9.1	9.1	0.2	83.6	12.7	1.91E+04
CFA-05	343660.0	4820999.0	-514.3	924.9	32.0	69.5	69.5	5.8	4829.2	27965.7	4.19E+07
CFA-05b	343590.7	4821014.8	-530.1	855.5	31.5	69.5	37.8	5.8	2626.4	15209.4	2.28E+07
CFA-52	342945.6	4821205.3	-720.5	210.5	13.5	3.5	2.4	2.9	8.4	24.4	3.65E+04
CFA-1709	342962.7	4821246.6	-761.8	227.5	13.8	2.3	2.1	2.6	4.9	12.8	n/a ³
CFA-2	343401.4	4828673.7	-8189.0	666.2	16.5	4.1	2.4	6.6	9.9	65.1	n/a
CFA-610	342945.3	4821255.3	-770.5	210.1	13.0	3.5	2.4	2.9	8.6	25.0	n/a
CFA-658	343251.3	4821242.8	-758.0	516.1	24.0	6.3	3.7	1.7	23.0	38.5	n/a
CFA-713-4	343043.9	4821050.1	-565.3	308.7	12.3	23.2	9.1	0.8	212.4	161.8	n/a
CFA-713-5	343047.6	4821054.8	-570.1	312.4	12.3	18.6	9.1	0.8	169.7	129.3	n/a
CFA-723	342988.1	4820973.1	-488.4	253.0	12.0	5.7	3.0	2.9	17.3	50.0	n/a
CFA-726	343109.0	4821080.0	-595.2	373.9	16.0	3.9	2.7	2.0	10.6	21.0	n/a
CFA-728	343126.9	4821130.0	-645.2	391.8	17.3	3.9	2.7	2.3	10.6	24.3	n/a
CFA-729	342973.5	4821251.1	-766.4	238.3	13.0	6.5	3.0	2.3	19.7	45.0	n/a
CFA-733	342988.1	4820973.1	-488.4	253.0	12.0	5.7	3.0	2.9	17.3	50.0	n/a

CFA-734	343002.9	4821284.7	-800.0	267.8	16.0	4.1	2.4	2.3	9.9	22.6	n/a
CFA-735	342909.2	4821326.3	-841.6	174.0	14.5	3.8	2.4	2.6	9.2	23.9	n/a
CFA-741-7	342988.1	4820973.1	-488.4	253.0	10.8	23.2	9.1	0.8	212.4	161.8	n/a
CFA-745	342950.3	4821123.8	-639.0	215.1	11.0	4.2	2.7	1.7	11.5	19.3	n/a
CFA-746	342878.1	4821146.6	-661.9	142.9	10.8	2.3	2.1	3.2	4.9	15.6	n/a
CFA-747	343290.2	4821837.0	-1352.3	555.0	47.0	4.6	2.7	4.7	12.5	59.3	n/a
CFA-748-B	342961.8	4821135.0	-650.3	226.6	11.0	4.2	2.7	1.7	11.5	19.3	n/a
CFA-750	342988.1	4820973.1	-488.4	253.0	12.0	5.7	3.0	2.9	17.3	50.0	n/a
CFA-46	342836.5	4821119.3	-634.6	101.4	12.00	5.8	5.8	6.9	33.2	228.9	n/a

1. UTM = Universal Transverse Meridian north and east coordinates in meters.

2. Offset = distance in meters of the center of each site from the center of the reference site (CFA-04) parallel and perpendicular to the groundwater flow direction. A negative value parallel to groundwater flow direction indicates the site is located upgradient of CFA-04. Positive values perpendicular to groundwater flow are sites to the east of CFA-04.

3. n/a = tanks identified in the Facility Analysis of the OU 4-13 Work Plan were modeled assuming one-tank volume of product released (see Table 6-8).

Contaminant inventories for these are based not on mass of contaminated soil but on mass contained in one tank volume. Tanks at sites CFA-26 and CFA-52 have petroleum inventory estimates based on this concept but also have sampling results which are used with estimates of contaminated soil mass to calculate contaminant inventories.

All tanks were modeled as parallelograms (right rectangles with uniform thickness) with dimensions that yield volumes equivalent to the original tank volume. Tank volumes are well-known data; records of the tank installation or removal provide adequate assessment of tank size. What is not well known for the tanks is the extent of contamination that may have resulted from the use of these tanks. Many were buried beneath land surface and it is not possible to provide with any assurance the actual contaminated volume of soil. As a result, the modeling effort assumes the tanks leaked one tank volume's worth of petroleum product. For the retained sites, sufficient soil sampling was performed to provide estimates of the depth and area of contaminated soil.

The computation of cumulative impacts to a common receptor from intermingling plumes that originate from different sources requires the introduction of a receptor network common to all the sites. CFA-04 was determined to be the most downgradient site, with respect to the groundwater flow direction. The center of this site was assumed to be the origin of the receptor grid coordinate system. As such, the center of CFA-04 was assigned the relative coordinates of (0, 0). GWMENU employs a Cartesian coordinate system with positive "X" direction in the direction of groundwater flow which is assumed, in the base case of this analysis, to be directly south. The "Y" direction is perpendicular to the groundwater flow and, in this case, is positive to the east.

A receptor grid was overlain on the source areas such that contributions to individual contaminant groundwater concentrations from all retained sites could be calculated at each receptor node. CFA-04 served as the most downgradient site, with respect to groundwater flow, and as such served as the model reference site. With the exception of CFA-12, CFA-04 is also the western-most site that was modeled. Contaminant groundwater concentrations were determined for each of ten receptor locations spread across an east-west line at the downgradient edge of CFA-04 that extends from 200 m (658 ft) west of the center of CFA-04 to 1200 m (3,947 ft) east of CFA-04. The modeled site dimensions, absolute coordinates, and relative coordinates of sites and receptors are presented in Table x1 and are shown graphically in Figure y1.

A common receptor grid allows groundwater concentrations of contaminants common to two or more sites to be summed for determining cumulative impacts. For each contaminant, groundwater concentrations were predicted for a receptor well located as part of the receptor grid network. Additionally, groundwater concentrations were predicted for a receptor well located in the center of the downgradient edge of each contamination site. The residential drinking water scenario at 100 years from the present is the primary focus of this analysis; as a result, maximum groundwater concentrations occurring at or before 100 years from the present were determined with the model.

The base case for comparison against all of the sensitivity analysis cases is the same as used for the original WAG 4 RI/BRA groundwater modeling. The contaminants modeled in the base case were also included in most of the sensitivity cases. Some contaminants did not yield any useful information for the sensitivity analysis; these were contaminants that did not reach a receptor at the receptor network or even a receptor located at the site's downgradient edge. These contaminants include very short-lived radionuclides or short-lived radionuclides with high adsorption factors. Table x2 summarizes the transport information for the contaminants that were modeled. Table x3 contains contaminants that were part of the original WAG 4 RI/BRA groundwater modeling that were not included in this sensitivity analysis.

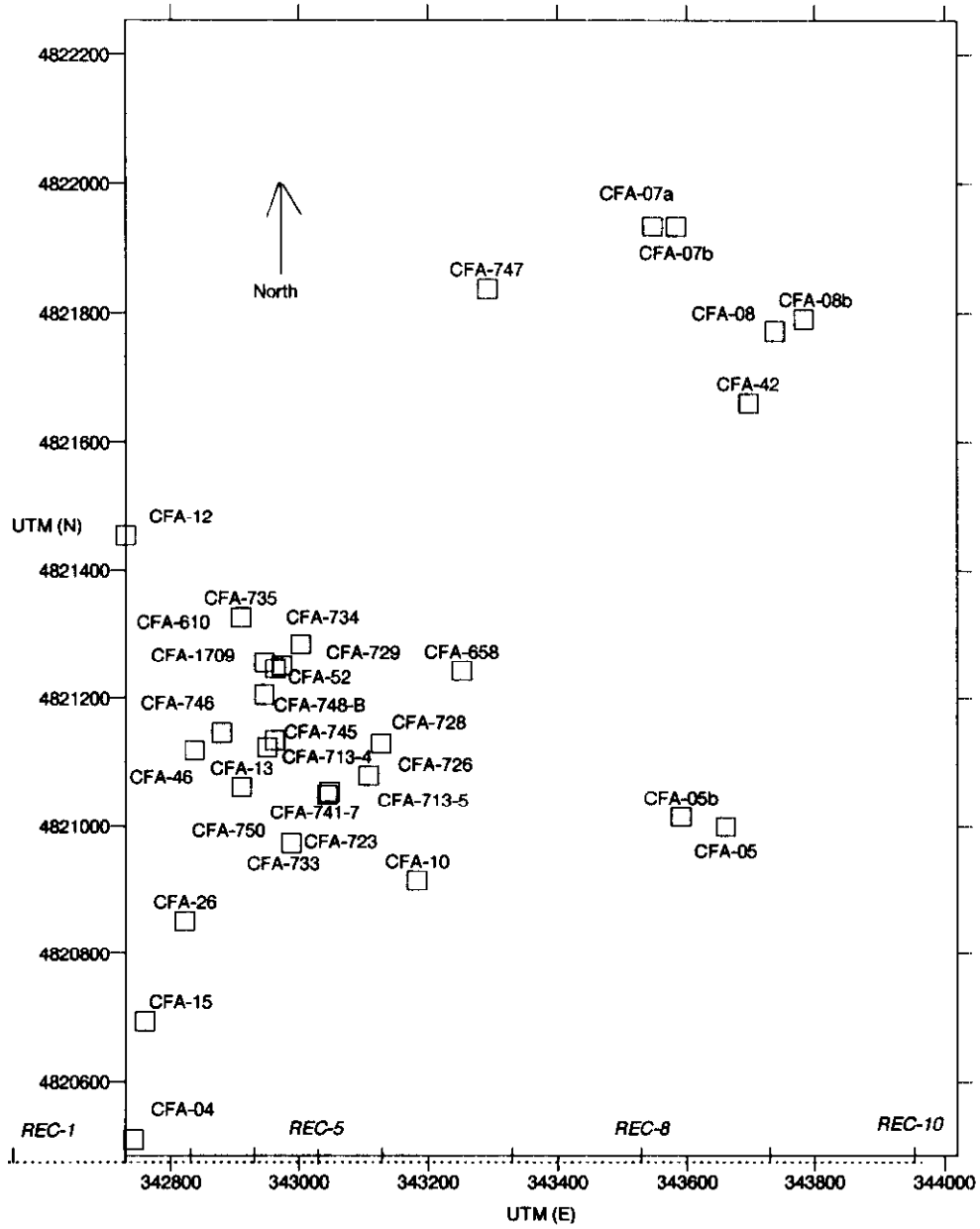


Figure y1. Modeled sites and receptor grid configuration (CFA-17, -47, and -2 not shown).

Table x2. Modeled contaminants and their properties.

Contaminant	Modeled Decay Product ^a	Half-life (yr)	Sorption Coefficient, Kd (mL/g) ^b	Total Inventory in Soil to be Transported to Groundwater (mg or Ci)
Ag-108m		1.27E+02	9.00E+01	4.80E-05
Am-241	Np-237	4.32E+02	3.40E+02	3.38E-02
				6.96E-06
Ba-133		1.05E+01	5.00E+01	4.73E-06
Eu-152		1.36E+01	0.00E+00	6.53E-05
Pu-238	U-234	8.78E+01	2.20E+01	7.12E-04
Pu-239/240		2.41E+04	2.20E+01	1.44E-02
Ra-226		1.60E+03	1.00E+02	2.95E-01
U-234		2.45E+05	6.00E+00	1.17E-01
U-235		7.04E+08	6.00E+00	5.93E-02
U-238		4.47E+09	6.00E+00	1.30E-01
Arsenic		n/a ^d	3.00E+00	7.49E+08
Benzo(a)anthracene		n/a	1.19E+03	3.58E+05
Benzo(b)fluoranthene		n/a	3.69E+03	1.67E+05
Benzo(g,h,i)perylene		n/a	4.74E+03	2.98E+05
Chlorodifluoromethane		n/a	1.73E-01	6.98E+05
Di-n-butylphthalate		n/a	1.02E+02	3.42E+06
Lead		n/a	1.00E+02	5.12E+09
Mercury		n/a	1.00E+02	5.53E+09
Phenanthrene		n/a	4.23E+01	8.11E+04
Phenol		n/a	8.64E-02	2.16E+05
Tetrachloroethene		n/a	7.89E-01	9.50E+02
1,1,1-Trichloroethane		n/a	3.27E-01	2.92E+02
TPH-diesel		n/a	1.78E+00	6.77E+10
TPH-gasoline			1.40E+00	4.90E+10
TPH-heating oil		n/a	1.78E+00	2.47E+11

a. Some parent radionuclides have relatively short half-lives and high sorption coefficients. For these (Ac-228, Am-241, Bi-214, and Pu-238), the first daughter product of these (Th-228, Np-237, Pb-210, and U-234, respectively) was modeled.

Daughter product inventories for these were obtained from the relationship of activity and half-life:
 $(\text{Activity})_{\text{daughter}} = (\text{Activity})_{\text{parent}} * \{(\text{half-life})_{\text{parent}} / (\text{half-life})_{\text{daughter}}\}$

b. For radionuclide contaminants with extremely short half-lives (i.e., less than 1.0 yr), the COCs are assumed to decay entirely to stable products before exiting the system. These contaminants were converted from parent curies to stable product milligrams (Pb-208 for thorium series decay chain COCs). The Pb-208 totals were added to the stable lead inventory for these sites before modeling.

c. Pb-208 is a stable form of elemental lead. The short-lived parent curies were converted to milligrams of Pb-208, which was added to the total lead inventory.

d. Half-life refers to radiological decay. Here, non-radiological COCs are considered to be free of any decay-type loss mechanisms.

Table x3. Contaminants not modeled.

Contaminant	Half-life (yr)	Sorption Coefficient, Kd (mL/g) ^b	Total Inventory in Soil to be Transported to Groundwater (Ci)
Ac-228	7.00E-04	0.00E+00	7.84E-02 2.87E-05
Bi-212	1.15E-04	1.00E+02	7.64E-02 4.38E-24
Bi-214	3.80E-05	1.00E+02	6.32E-02 1.14E-07
Cs-137	3.02E+01	5.00E+02	7.63E+00
Pb-212	1.21E-03	1.00E+02	8.03E-02 4.85E-23
Tl-208	5.80E-06	0.00E+00	7.32E-02 2.12E-25
Zr-95	1.75E-01	6.00E+02	1.75E-01

CUMULATIVE VADOSE ZONE SEDIMENT THICKNESS

The existing modeling was prepared using the GWMENU user-interface for the GWSCREEN model code. GWSCREEN refers to the unsaturated zone thickness as a parameter called "depth." This parameter encompasses the total vertical distance in the unsaturated zone between the bottom of a contamination source and the top of the aquifer. The unsaturated zone beneath the INEEL is a stratified sequence of solidified basalt flows that are occasionally separated by sediment deposits of windblown, fluvial, or lacustrine origin. However, it is typical for risk assessment of the groundwater pathway to ignore any retentive effects of basalt sequences. It is believed that significant fracturing in these brittle flows allows very rapid vertical transmission of water and water-borne contaminants in the vadose zone. Beneath the INEEL, sediments typically only comprise 10% of the entire vadose zone depth.

The unsaturated zone is comprised of basalt sequences separated by sediment deposits. The sedimentary interbeds, although typically thinner than the basalt layers, represent deposition during long periods of volcanic quiescence. These sediments were deposited by various mechanisms and are of diverse origins. The sediments in the CFA area consist of fine-grained silts delivered by wind and silts, sands, and coarse gravels deposited by fluvial action. All source areas are assumed to be underlain by sedimentary interbeds of varying thickness. The total unsaturated sediment thickness includes interbeds above the aquifer as well as the surficial sediment thickness that occurs at land surface. Obviously, the value is expected to vary spatially. The mechanisms that deposited the interbeds and those that produced basalt flows were not consistent and did not leave behind ideally uniform interbed and flow thicknesses.

The selection of a value for the "depth" parameter is usually found by summing the separating sediment thicknesses beneath a given site based on subsurface lithology data gleaned from well logs and drilling notes. For the original WAG 4 RI/BRA modeling, site-specific values of unsaturated zone total sediment thickness were determined from isopleths generated using a Kriging interpolation routine. The data for the kriging were obtained from 12 aquifer wells at or near CFA. This sensitivity analysis expanded the number of wells to 64. This increased the area examined to help identify any spatial trends in unsaturated sediment thickness. The wells included in the sensitivity analysis and their cumulative vadose zone sediment thickness values are presented in Table x4. The unsaturated sediment thickness values in Table x4 are summarized in Table x5.

Table x4. Wells included in unsaturated zone sediment thickness analysis.

Well	Northing	Easting	Land surface (m above MSL)	Cumulative vadose zone sediment thickness (m) (average)	Depth to water (m)	Percentage of vadose zone that is sediment
CFA-1	681602.51	295252.24	1499.6	39.6	142.4	28
CFA-2	679599.87	294085.52	1500.5	16.3	143.3	11
CFA-MON-A-001	675528.01	293001.57	1502.1	16.0	149.7	11
CFA-MON-A-002	675602.34	294701.00	1500.8	17.2	148.5	12
CFA-MON-A-003	675593.81	296205.20	1500.2	28.7	148.1	19
CPP-01	696665.09	296666.17	1494.7	30.3	136.6	22
CPP-02	696664.56	296167.92	1495.1	23.3	137.5	17
CPP-03	694817.28	296573.65	1495.9	24.0	137.2	18
CPP-04	697486.48	297949.17	1493.8	23.0	134.2	17
EOCR PRODUCTION WELL	677080.67	306146.76	1503.1	6.2	147.3	4
HIGHWAY 3	687065.16	277159.41	1515.9	47.1	164.0	29
LF2-08	682878.46	294360.90	1500.7	25.2	146.0	17
LF2-09	682899.02	294198.77	1500.8	24.5	146.9	17
LF2-10	682830.95	294273.15	1500.9	17.9	146.5	12
LF2-11	684290.87	295462.44	1499.6	26.5	144.1	18
LF2-12	682927.00	294023.75	1501.0	17.3	146.7	12
LF3-08	683111.45	291542.85	1503.3	19.3	148.3	13
LF3-09	682824.23	291516.45	1503.5	16.3	148.0	11
LF3-10	683528.93	290880.55	1504.0	30.2	148.5	20
LF3-11	686244.26	292688.22	1501.4	22.7	148.0	15
OMRE	676726.96	306498.90	1502.1	8.7	152.1	6
RIFLE RANGE WELL	685751.97	282883.08	1511.6	25.3	154.1	16
SITE-09	677323.04	309855.57	1498.9	11.2	143.7	8
TRA-03	701617.16	289956.57	1496.8	47.8	138.9	34
TRA-04	701708.95	289417.36	1495.1	21.8	140.9	15
TRA-05A	698839.00	288820.00	1499.2	32.6	145.1	22
TRA-06A	698072.00	288957.00	1498.8	29.5	143.0	21
TRA-07	698378.29	288103.76	1500.6	29.6	144.2	21
TRA-08	696555.86	287904.98	1501.7	45.9	145.1	32
TRA DISPOSAL	700116.31	289723.16	1499.1	32.7	143.0	23
USGS-020	686506.58	301198.75	1496.0	18.8	139.5	13
USGS-034	690800.41	292742.89	1499.9	17.8	142.1	12
USGS-035	691251.79	292498.68	1500.0	21.0	143.0	15
USGS-036	690359.70	292981.03	1499.9	33.2	142.9	23
USGS-037	689921.26	293222.65	1500.0	38.3	143.0	27
USGS-038	689568.16	293578.01	1500.0	26.2	143.2	18
USGS-039	691691.35	292260.97	1500.4	38.4	143.6	27
USGS-040	694540.46	295937.87	1495.9	37.8	138.9	27
USGS-041	694138.95	295938.92	1496.2	35.3	139.1	25
USGS-042	693638.23	295938.30	1496.5	25.5	139.3	18
USGS-043	694858.82	295721.85	1495.9	38.9	138.8	28
USGS-044	694236.83	295250.28	1496.5	24.2	139.4	17
USGS-045	693600.77	295493.96	1496.6	31.5	139.2	23
USGS-046	694024.25	295724.38	1497.7	27.6	138.4	20
USGS-047	694113.87	296575.88	1496.0	25.6	137.9	19
USGS-048	693415.70	296614.30	1496.2	26.7	138.5	19

USGS-049	693642.17	297234.09	1495.3	27.9	138.1	20
USGS-051	692343.41	296343.72	1496.7	22.8	139.2	16
USGS-052	694832.51	297971.18	1493.9	39.8	138.7	29
USGS-057	691752.88	294869.97	1497.9	25.8	141.5	18
USGS-059	692767.88	297675.38	1495.1	34.2	138.9	25
USGS-067	691727.50	298203.50	1495.3	24.7	138.9	18
USGS-077	688822.47	296494.36	1497.6	18.4	142.1	13
USGS-082	693412.02	300455.28	1493.1	27.6	136.6	20
USGS-083	671394.05	295470.22	1503.7	18.2	151.6	12
USGS-084	693067.82	289297.77	1502.6	27.0	146.6	18
USGS-085	685931.54	291435.45	1503.0	20.7	147.1	14
USGS-104	662584.67	295915.14	1518.0	16.4	169.2	10
USGS-111	690434.67	296389.79	1497.3	13.6	141.5	10
USGS-112	688765.27	294492.92	1499.5	24.5	142.6	17
USGS-113	688760.32	295409.70	1498.7	16.8	143.0	12
USGS-114	689180.42	297441.72	1497.1	17.0	141.3	12
USGS-115	689310.47	298132.39	1496.8	15.6	140.2	11
USGS-116	690452.31	298785.17	1495.9	19.5	138.4	14

Table x5. Summary statistics for WAG 4 unsaturated zone sediment thickness

number of wells analyzed	average vadose zone sediment thickness (m)	minimum vadose zone sediment thickness (m)	maximum vadose zone sediment thickness (m)	standard deviation
64	25.5	6.2	47.8	9.0

The data used to prepare the values in Table x4 were obtained from several sources drillers' notes, well log libraries, and electronic lithology databases (Sehlke et al., 1993; Anderson, et al., 1996; LMITCO Hydrologic Data Repository). If the different references yielded different unsaturated zone sediment thickness values for the same well, the average of these different values was determined and is presented in Table x4.

Figure y2 shows the location of the wells used in the sediment thickness analysis. Figure y3 presents the average vadose zone sediment thickness value from Table x4. Contours were prepared for Figure y3 without the use of kriging or other interpolation techniques. This was done to more clearly indicate any spatial trend. The contours indicate the unsaturated sediment thickness tapers toward the southeast of CFA. This probably indicates the Big Lost River, which is near areas in Figure y3 that have thicker unsaturated sediment thickness, is the dominant depositional mechanism in the area.

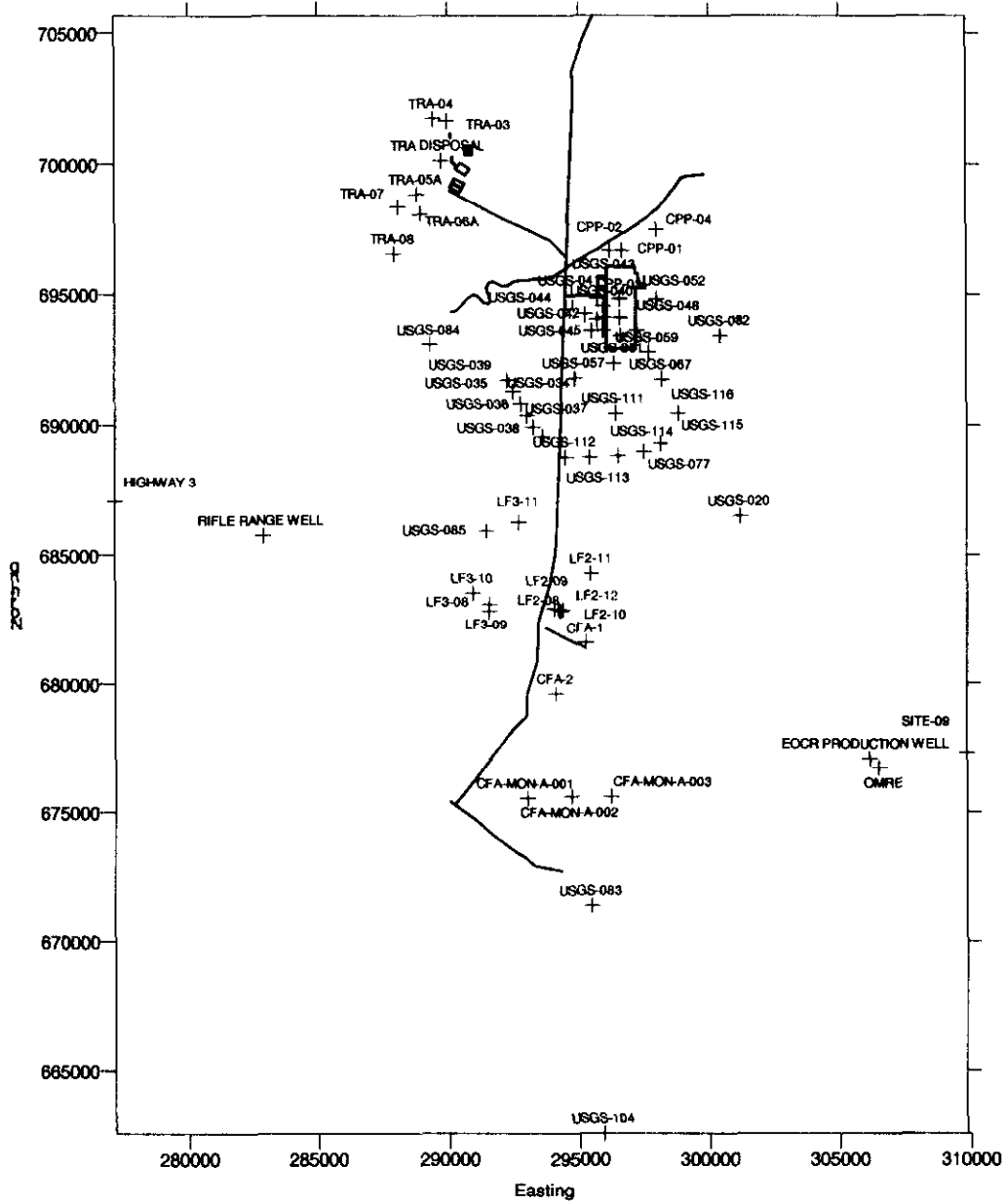


Figure y2. Location of wells included in unsaturated zone sediment thickness analysis.

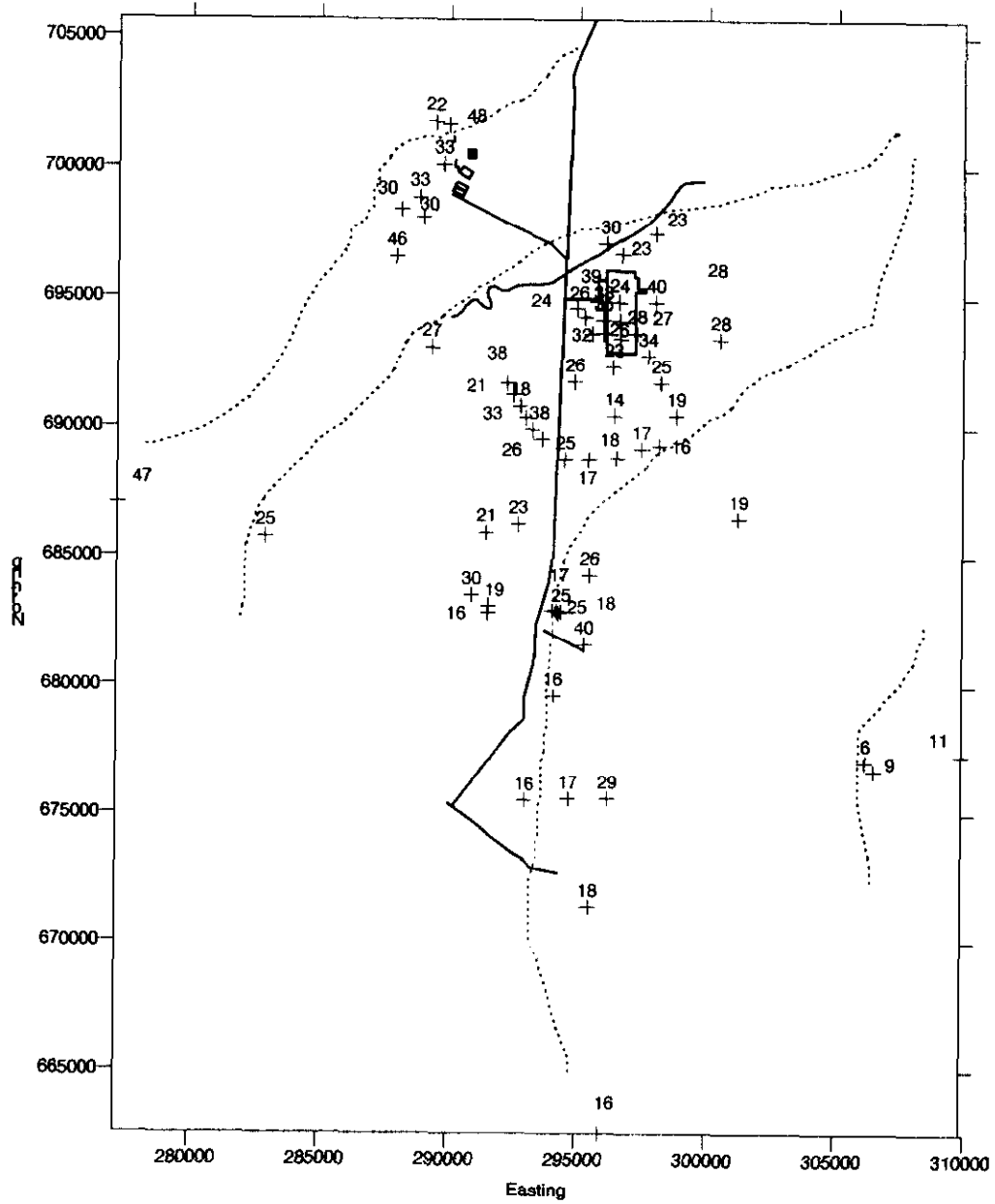


Figure y3. Unsaturated zone sediment thickness values (m) and possible thickness contours.

In the original WAG 4 RI/BRA groundwater model, sites were assigned a unique unsaturated sediment thickness determined from the contours of 12 wells' kriged lithology data. In this sensitivity analysis, a single unsaturated zone sediment thickness value was assigned to all WAG 4 sites for each of two sensitivity cases. Case 1 uses a value of 6.2m which is the minimum of the 64 wells in Table x4; this value is assumed to be a reasonable minimum sediment thickness. Figure y3 indicates the interbeds become thinner toward the southeast of CFA; however, it may not be reasonable to assume they thin to nothing beneath much of WAG 4. As a check against this possibility, an additional sensitivity analysis case was examined in which all sites were assigned an unsaturated sediment thickness of 1.0 m.

Table x6 lists the unsaturated sediment thickness value for each site as originally modeled and also shows the percentage by which the case 1 (6.2 m) and case 2 (1.0 m) values differ from the original values. Case 1 (6.2m) represents an average decrease in sediment thickness of 70% for the modeled sites. Case 2 (1.0 m) is an average 95% decrease in originally modeled unsaturated sediment thickness.

Note in the summary statistics at the bottom of Table x6 that the average unsaturated sediment thickness used in the WAG 4 RI/BRA modeling of the retained sites (i.e., base case) is in good agreement with the average thickness value determined from analysis of 64 wells (see Table x5). The average unsaturated sediment thickness appears stationary with respect to the size of the area examined.

Table x6. Base case values and sensitivity analysis values of sediment thickness for each site

Site	Base case unsaturated zone sediment thickness (m)	Case 1 unsaturated zone sediment thickness (m)	% change from base case	Case 2 unsaturated zone sediment thickness (m)	% change from base case
CFA-04	14.0	6.2	-56	1.0	-93
CFA-05	32.0	6.2	-81	1.0	-97
CFA-05b	31.5	6.2	-80	1.0	-97
CFA-07a	46.3	6.2	-87	1.0	-98
CFA-07b	46.3	6.2	-87	1.0	-98
CFA-08	47.0	6.2	-87	1.0	-98
CFA-08b	49.0	6.2	-87	1.0	-98
CFA-10	19.0	6.2	-67	1.0	-95
CFA-12	12.9	6.2	-52	1.0	-92
CFA-13	14.0	6.2	-56	1.0	-93
CFA-15	13.5	6.2	-54	1.0	-93
CFA-17a	18.5	6.2	-66	1.0	-95
CFA-17b	18.5	6.2	-66	1.0	-95
CFA-26	13.0	6.2	-52	1.0	-92
CFA-42	40.9	6.2	-85	1.0	-98
CFA-47	18.5	6.2	-66	1.0	-95
CFA-52	13.5	6.2	-54	1.0	-93
Summary statistics					
average	26.4		-70		-95
minimum	12.9		-87		-98
maximum	49.0		-52		-92

The results of new GWMENU simulations using the case 1 and case 2 unsaturated sediment thicknesses for each site are presented in Tables x7 through x10. These tables present only concentrations predicted to occur during the 100-year timeframe. Concentrations that are predicted to occur in the future after the 100 year timeframe are not included. Table x7 shows concentrations occurring at receptors that are part of the receptor network located downgradient of CFA-04.

Table x7. Maximum 100-yr groundwater concentrations at receptor grid locations

Contaminant	BASE CASE		CASE 1 (unsaturated sediment=6.2m)				CASE 2 (unsaturated sediment=1.0m)			
	Concentration (mg/L or pCi/L)	Time of arrival (yr)	Concentration (mg/L or pCi/L)	%change in concentration from base case	Time of arrival (yr)	%change of time from base case	Concentration (mg/L or pCi/L)	%change in concentration from base case	Time of arrival (yr)	%change of time from base case
Chlorodifluoromethane	1.7E-04	7.8E+01	1.7E-04	0	4.0E+01	-49	1.7E-04	0	1.1E+01	-86
Eu-152	4.8E-03	4.1E+01	1.3E-02	178	2.1E+01	-49	3.0E-02	516	5.4E+00	-87
Phenol	7.1E-05	5.9E+01	7.1E-05	0	3.0E+01	-49	7.1E-05	0	7.6E+00	-87
1_1_1-Trichloroethane	6.2E-08	1.2E+02	6.2E-08	0	6.3E+01	-48	6.2E-08	0	2.1E+01	-82

Note that the maximum concentrations occurring during the 100-year timeframe do not change regardless of the unsaturated sediment thickness value. The arrival time, however, is significantly influenced by the unsaturated sediment thickness value. The travel time appears to be directly proportional to the unsaturated sediment thickness which correlates well with equation 21 of p.16 of the GWSCREEN User's Manual (Rood, 1994). The equation shows that transit time in the unsaturated zone is directly proportional to both unsaturated zone thickness and the contaminant retardation coefficient but inversely proportional to the unsaturated pore velocity. For case 1, the 6.2m thickness is about 50% less than the originally modeled thicknesses for the sites in Table x7. This results in about a 50% reduction in the arrival times of the maximum concentrations. Similarly, the approximately 90% thickness reduction in case 2 results in about 90% reduction of the maximum concentration arrival times.

With the thinner unsaturated sediment thicknesses, the model predicts several new contaminants will reach the receptor network during the 100-year timeframe. These are shown in Table x8. These did not pose any groundwater threat when the unsaturated sediment thickness was 6.2m or one of the base case values. Tetrachloroethene, however, is predicted to appear at a receptor well during the 100-year timeframe for the 6.2 m case. This contaminant has a very low adsorption coefficient (0.789). The arrival time of the maximum 100-year concentration for several contaminants occurs between 100 and 130 years. The analysis of the 100-year timeframe included a 30-year averaging window (100-130 years from present). Those with arrival times at exactly 130 years are increasing in concentration and will peak at some time beyond 130 years.

Table x8. 100-year receptor well groundwater concentrations unique to worst-case sediment thickness

Contaminant	Modeled contaminant or daughter product	Receptor	Concentration (mg/L or pCi/L)	Time of arrival (yr)
Arsenic		2	4.4E-02	72
TPH-gasoline		5	1.6E+00	130
TPH-diesel		4	2.5E+00	130
TPH-heating oil		6	1.5E+00	130
Am-241	Np-237	9	2.7E-09	130
	U-233		1.3E-12	
	Th-229		4.7E-16	
U-234	U-234	2	3.5E+00	130
	Th-230		2.5E-03	
	Ra-226		6.9E-05	
	Pb-210		4.3E-05	
U-235	U-235	2	2.5E-01	130
	Pa-231		4.8E-04	
	Ac-227		4.2E-05	
U-238	U-238	2	3.8E+00	130
	U-234		1.4E-03	
	Th-230		5.1E-07	
	Ra-226		9.4E-09	
	Pb-210		5.0E-09	
Tetrachloroethene		4	1.1E-07	120
		4	1.1E-07	44

Tetrachloroethene appeared as new groundwater contaminant for both cases (6.2 and 1.0m) of

unsaturated sediment thickness; presented here are the results for both 6.2m (120 years) and 1.0m case (44 years), respectively.

The concentrations in Table x7 and x8 are predicted to occur at the receptor network depicted in Figure y1. Table x9 presents concentrations predicted for the groundwater immediately beneath each site. Again, these concentrations are the only ones predicted to occur in the 100-year timeframe. Locating the receptor well at the site's edge ignores the travel time in the aquifer and the dispersion associated with groundwater transport. This modeling effort did not include dispersion in the unsaturated zone but treated vadose zone transport as "plug" flow. Even without the aquifer travel time and dispersion, only one additional contaminant (Pu-238) appears in the groundwater beneath the sites that is not predicted at the receptor network.

Table x9 presents predicted concentrations for the daughter products of some of the heavier isotope contaminants. Pu-238 and Am-241, because of their relatively short half-lives, are modeled as their first daughter products, U-234 and Np-237, respectively. Note the high predicted groundwater concentrations of U-234 and U-238 (modeled as U-234). These occur in receptor well location number 2. The receptor grid is located along the downgradient edge of the most-downgradient site, CFA-04. Receptor well number 2 is located directly along the edge of CFA-04. CFA-04 contains approximately 0.1 Ci each of U-238 and U-234. As expected, the groundwater concentrations from beneath CFA-04 (Table x9) are the same as in receptor well number 2 (Table x8).

Table x9. Maximum 100-year groundwater concentrations beneath site locations

Contaminant	Site	Base Case		Case 1 (6.2 m)			Case 2 (1.0m)			
		Concentration (mg/L or pCi/L)	Time of arrival (yr)	Site	Concentration (mg/L or pCi/L)	Time of arrival (yr)	Site	Modeled parent or daughter	Concentration (mg/L or pCi/L)	Time of arrival (yr)
Chlorodifluoromethane	CFA-26	6.7E-04	73	CFA-26	6.7E-04	36	CFA-26	n/a	6.7E-04	7
Eu-152	CFA-12	8.6E-02	39	CFA-12	2.4E-01	19	CFA-12	n/a	5.3E-01	3
Phenol	CFA-26	2.7E-04	57	CFA-26	2.7E-04	27	CFA-26	n/a	2.7E-04	5
1_1_1-Trichloroethane	CFA-52	9.9E-07	108	CFA-52	1.0E-06	50	CFA-52	n/a	1.0E-06	9
Tetrachloroethene	n/a	0	n/a	CFA-52	1.7E-06	94	CFA-52	n/a	1.7E-06	17
Arsenic	n/a	0	n/a	n/a	0	n/a	CFA-04	n/a	4.4E-02	72
Am-241							CFA-05a	Np-237	1.3E-04	125
								U-233	5.9E-08	n/a
								Th-229	2.1E-11	n/a
Pu-238	n/a	0	n/a	n/a	0	n/a	CFA-07a	U-234	3.0E-05	125
								Th-230	2.1E-08	n/a
								Ra-226	5.5E-10	n/a
								Pb-210	3.4E-10	n/a
U-234	n/a	0	n/a	n/a	0	n/a	CFA-04	U-234	3.5E+00	130
								Th-230	2.5E-03	n/a
								Ra-226	6.9E-05	n/a
								Pb-210	4.3E-05	n/a

Table x10. At-site 100-year groundwater concentration arrival time comparison

Contaminant	Site	Base case			Case 1				Case 2			
		Concentration at site edge (mg/L or pCi/L)	Base case sediment thickness (m)	Time of arrival (yr)	Case 1 sediment thickness (m)	% change from base case	Time of arrival (yr)	%change in arrival time from base case	Case 2 sediment thickness (m)	% change from base case	Time of arrival (yr)	%change in arrival time from base case
Chlorodifluoromethane	CFA-26	6.7E-04	13	73	6.2	-52	36	-51	1.0	-92	7	-91
Phenol	CFA-26	2.7E-04	13	57	6.2	-52	27	-52	1.0	-92	5	-91

1_1_1-Trichloroethane	CFA-52	9.9E-07	13.5	108	6.2	-54	50	-54	1.0	-93	9	-92
-----------------------	--------	---------	------	-----	-----	-----	----	-----	-----	-----	---	-----

Table x10 compares the arrival times for the three non-radiological contaminants that appear in the groundwater beneath the source site for each of the three unsaturated sediment thickness cases. For all three cases, the concentrations of each contaminant in the groundwater beneath the sites is the same. The arrival times do change per changes in unsaturated zone sediment thickness. The changes in arrival times appear to be in direct proportion to changes in the cumulative vadose zone sediment thickness.

Eu-152 is the one radiological contaminant that arrives in the groundwater for each of the three sediment thickness cases during the 100-year timeframe. The contaminant was modeled with an adsorption factor of 0.0, an INEEL Track 2 default value. An adsorption factor greater than 0.0 will probably bind this relatively short-lived (13.6 year half-life) isotope to the sediments in the vadose zone beneath the source site until the contaminant decays to a stable product.

However, Table x11 provides information on the sensitivity of groundwater concentrations to changes in the cumulative unsaturated zone sediment thickness. Non-radiological contaminants will eventually achieve an equilibrium concentration regardless of the sediment thickness as long as there is a force (infiltration) driving the contaminant to the aquifer. Radiological contaminants, as seen for Eu-152 in Table x11, achieve very different peak concentrations in the aquifer depending on the sediment thickness, the contaminant adsorption factor, and its half-life.

Table x11. 100-year groundwater concentration for radiological contaminant (Eu-152)

Case	Unsaturated sediment thickness (m)	%change from base	Concentration at site edge (mg/L or pCi/L)	%change from base	Time of arrival (yr)	%change from base
Base	12.9	n/a	8.6E-02	n/a	39	n/a
Case 1	6.2	-52	2.4E-01	179	19	-52
Case 2	1	-92	5.3E-01	516	3	-92

GROUNDWATER FLOW DIRECTION

In the original WAG 4 RI/BRA modeling, the groundwater was assumed to flow directly south. This simplified construction of the groundwater model. The actual groundwater flow direction beneath CFA is believed to be to the southwest since that is the direction of groundwater flow most observed across the rest of the INEEL. Water table contours for the aquifer beneath the INEEL are presented in the main text of the WAG 4 RI/BRA. They show that the regional flow beneath the INEEL is south-southwest, although the local direction of groundwater flow may be affected by recharge from streams, surface water spreading areas, and inhomogeneities in the aquifer.

The groundwater flow direction was examined in this analysis by plotting contours of groundwater elevation to determine the direction of maximum elevation gradient. The aquifer wells and their water levels used in this analysis are provided in Table x12. A contour plot for the central INEEL area is shown in Figure y4 for October 1995. More recent data was available for the wells in the CFA area. These are plotted in Figures y5 which shows groundwater elevations for April 1998. The October 1995 "bigger" picture is easier to plot contours on; however, the CFA area shows contradicting elevations (i.e., wells suspected of being downgradient per the southwest direction have higher elevations than upgradient wells) indicating the groundwater flow may be anything but southwest.

Table x11. Wells and water levels used in analysis of groundwater gradients

Well	Northing	Easting	Oct-95	Dec-96	Aug-97	Apr-98
Lf 2-10	682830.9	294273.1	ND	4451.7	4455.4	4454.0
LF 2-11	684290.9	295462.4	ND	4453.6	4454.3	4456.9
LF 2-9	682899.0	294198.8	ND	4454.1	4455.8	4457.3

LF 3-10	683528.9	290880.6	ND	4453.8	4455.3	4456.8
LF 3-8	683111.4	291542.8	ND	4455.7	4458.6	4458.5
LF 3-9	682824.2	291516.4	ND	4453.8	4455.2	4456.8
LF2-8	682878.5	294360.9	ND	4453.8	4459.3	4457.0
Site 9	677337.7	309840.6	4453.9	ND	ND	ND
USGS 1	650501.2	335650.6	4434.5	ND	ND	ND
USGS 17	727253.8	315177.0	4475.1	ND	ND	ND
USGS 20	686506.6	301198.8	4451.9	4451.5	4452.9	4454.3
USGS 22	695930.6	264348.6	4436.1	ND	ND	ND
USGS 23	735554.3	279549.6	4478.6	ND	ND	ND
USGS 34	690800.4	292742.9	4454.1	4454.3	4455.6	4457.1
USGS 35	691251.8	292498.7	ND	4455.7	4457.0	4458.5
USGS 36	690359.7	292981.0	ND	4454.3	4455.7	4457.2
USGS 37	689921.3	293222.6	4454.1	4454.3	4455.6	4457.0
USGS 38	689568.2	293578.0	ND	4454.6	4455.7	4457.2
USGS 39	691691.3	292261.0	4453.6	4454.1	4457.7	4457.2
USGS 40	694472.4	295999.4	4453.9	ND	ND	ND
USGS 48	693453.8	296652.7	4454.2	ND	ND	ND
USGS 5	703512.4	325031.4	4466.4	ND	ND	ND
USGS 57	691752.9	294870.0	4453.9	4453.8	4455.6	4457.1
USGS 59	692734.9	297750.5	4455.2	ND	ND	ND
USGS 67	691717.7	298256.6	4457.0	ND	ND	ND
USGS 77	688822.5	296494.4	4454.0	4453.7	4455.4	4457.0
USGS 82	693412.0	300455.3	4455.3	4454.6	4456.2	4457.8
USGS 83	671394.1	295470.2	4442.3	ND	ND	ND
USGS 84	693118.0	289286.5	4454.1	ND	ND	ND
USGS 85	685931.5	291435.5	ND	4454.0	4455.5	4457.0
USGS 97	718307.0	300209.7	4472.7	ND	ND	ND
Water Supply for INEL #1	713220.4	294334.0	4476.7	ND	ND	ND
USGS 104	662577.5	295925.5	4433.9	ND	ND	ND
USGS 104	662584.7	295915.1	4433.5	ND	ND	ND
USGS 106	669059.4	280994.0	4428.1	ND	ND	ND
USGS 107	667130.9	307797.2	4437.9	ND	ND	ND
USGS 111	690434.7	296389.8	ND	4454.2	4455.7	4456.5
USGS 112	688765.3	294492.9	ND	4454.5	4455.8	4457.7
USGS 113	688760.3	295409.7	ND	4455.1	4457.8	4458.0
USGS 114	689180.4	297441.7	ND	4454.3	4457.5	4457.2
USGS 115	689310.5	298132.4	ND	4454.8	4457.0	4457.1
USGS 116	690452.3	298785.2	ND	4455.2	4456.9	4457.7

ND = no data available for this well on this date

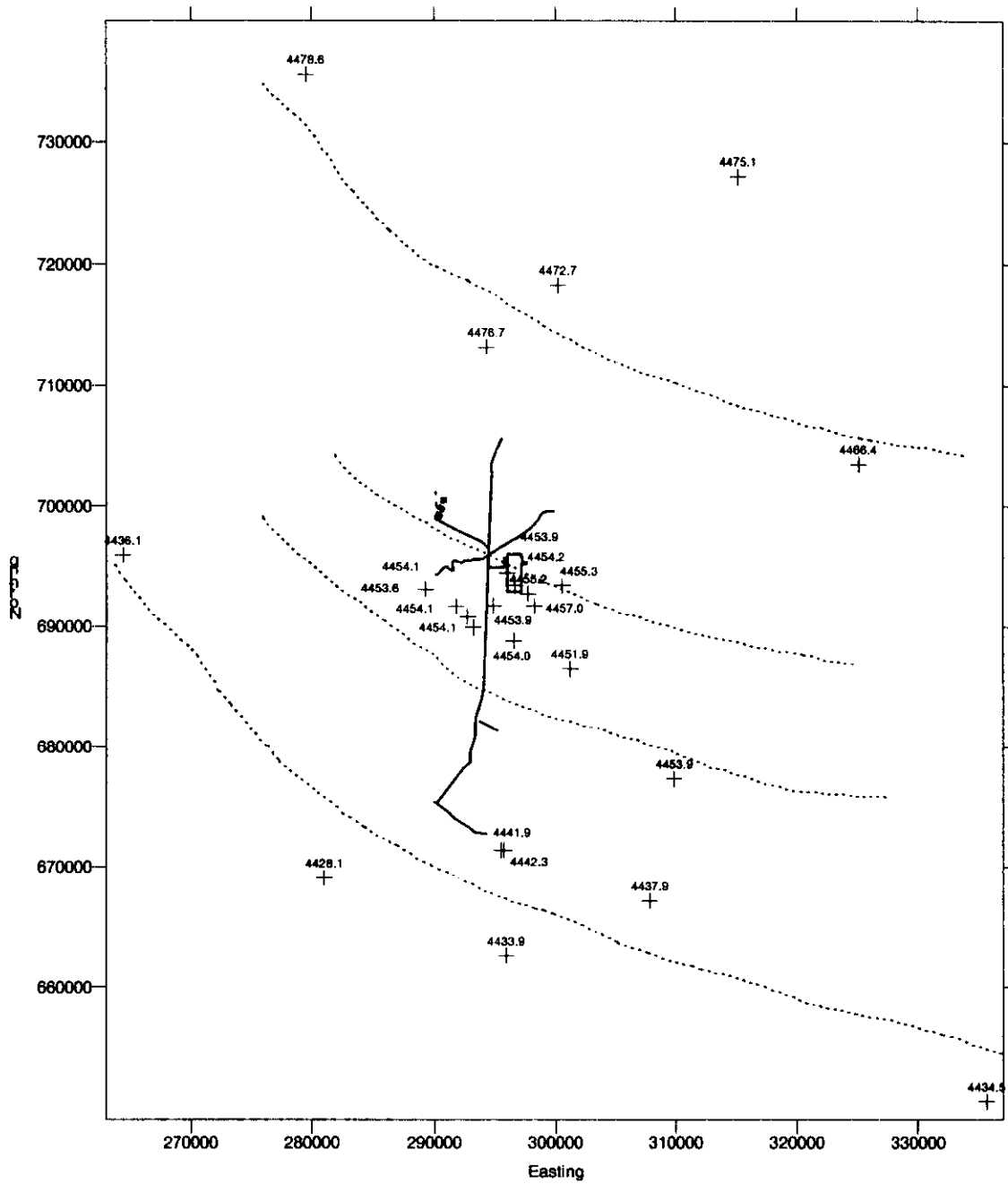


Figure y4. Groundwater levels for central INEEL, October 1995

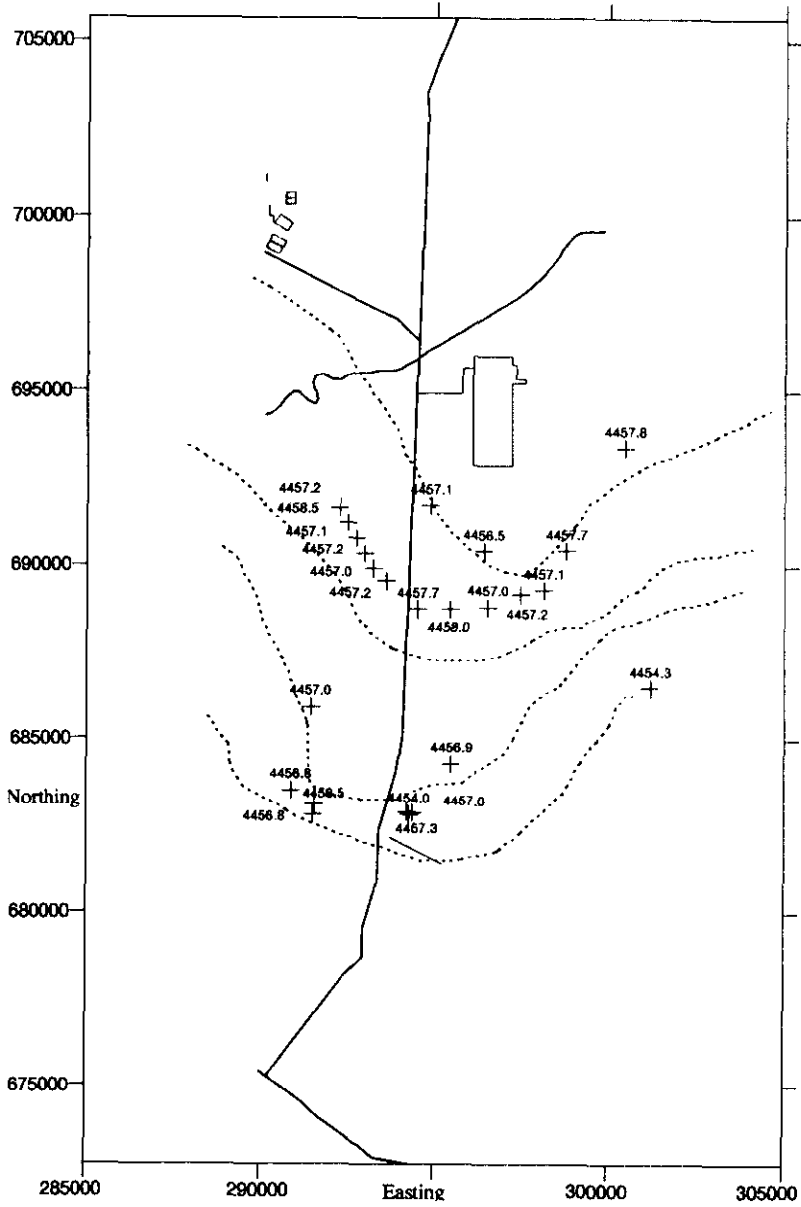


Figure y5. Groundwater levels for CFA, April 1998

To avoid gathering additional groundwater elevation data, it was determined that modeling the groundwater flow direction as directly south and directly west would be sufficient for the sensitivity analysis. To simulate the groundwater flow as 90 degrees off of the original model, the dimensions Length and Width for each source site were switched. Then, the receptor network was rotated 90 degrees counterclockwise (from above) while maintaining CFA-04 as the network origin (GWSCREEN does not specify a groundwater flow direction but is implied by the Length and Width and receptor grid).

The resulting maximum 100-year groundwater concentrations at both the receptor locations and beneath the source sites are presented in Table x12 along with the equivalent for the base case. Since CFA-04 is maintained as the reference site and the unsaturated zone sediment thickness values are the same as for the base case, it is not surprising that the resulting contaminant concentrations are roughly the same. No new contaminants appear at either the receptor network or the site locations as a result of the flow change. The contaminant shown in Table x12 have the lowest adsorption factors of all contaminants modeled. They are the least affected by changes in unsaturated zone thickness, site dimensions, or groundwater flow direction.

Table x12. 100-year groundwater concentrations for different flow directions

COC	Base case (groundwater flow directly south)			Case 3 (groundwater flow directly west)			
	Site or receptor	Concentration (mg/L or pCi/L)	Arrival time (yr)	Concentration (mg/L or pCi/L)	% change from base case	Arrival time (yr)	%change from base case
at site's edge							
Chlorodifluoromethane	CFA-26	6.7E-04	73	6.7E-04	0	74	1
Eu-152	CFA-12	8.6E-02	39	8.6E-02	0	39	0
Phenol	CFA-26	2.7E-04	57	2.7E-04	0	56	0
1_1_1-Trichloroethane	CFA-52	9.9E-07	108	1.0E-06	0	108	0
at receptor grid							
Chlorodifluoromethane	3	1.7E-04	78	1.9E-04	12	75	-4
Eu-152	2	4.8E-03	41	3.9E-03	-18	39	-5
Phenol	3	7.1E-05	59	7.9E-05	11	57	-3
1_1_1-Trichloroethane	4	6.2E-08	120	2.3E-08	-62	112	-7

GWSCREEN VERIFICATION

To achieve estimates of cumulative concentrations resulting from separate groundwater plumes of the same contaminant, the user-interfacing GWMENU version of GWSCREEN was employed. This version allows incorporation of receptor network via a common spatial coordinate origin. The same could be accomplished with other versions of GWSCREEN if the user is willing to prepare separate runs for each receptor at the receptor network and to determine these common receptors' locations relative to each site. GWMENU simplifies that step but uses the same solution algorithm as GWSCREEN version 2.4a, which is well-documented (Rood, 1994).

To ensure that the two versions produce similar if not the same results, runs were made with the two codes for a subset of the base case using the same sites, contaminants, and receptor locations. The results are presented in Table x13 and the negligible differences between the two sets indicate the code versions do produce very similar results.

The same parameter values were used for both versions of the code. Note that for almost every site and contaminant the resulting peak concentrations and arrival times are nearly identical. A small amount of difference is to be expected; predictions of groundwater concentration made by a semi-analytical screening tool should never be regarded as extremely accurate or precise. The results in Table x13 are identical to the first significant digit. There exists great uncertainty in almost every parameter used in groundwater risk assessment; therefore, precision of results much beyond the first significant digit should not be trusted much.

Table x13. Comparison of GWMENU and GWSCREEN version 2.4a results

Case	Site	Contaminant	Initial inventory (mg)	Groundwater concentration beneath site (mg/L)	%Difference in concentration from base case
Base	CFA-26	Phenol	2.16E+05	2.7E-04	
Case 4	CFA-26	Phenol	2.16E+05	2.5E-04	7%

SUMMARY

This sensitivity analysis of the WAG 4 RI/BRA groundwater modeling included examining how predicted groundwater concentrations are affected by changes in unsaturated sediment thickness, groundwater flow direction, and GWSCREEN code version. The results using a central INEEL minimum unsaturated zone sediment thickness of 6.2m and those using a thickness of 1.0m were compared to the base case, original modeling results. Resulting groundwater concentrations using a flow direction to the south were compared with results from simulating the groundwater flow direction to the west.

The results of the vadose zone thickness analysis indicate that the magnitude of the groundwater concentrations of non-decaying contaminants is not affected by changes in this parameter; hence, the associated risk or hazard quotient, of non-radiological contaminants, will remain the same regardless of changing this parameter.

The time at which the peak concentration arrives at the receptor location is, however, strongly dependent on this parameter and appears to be directly proportional. Arrival times with the 6.2 m thickness value were all about 50% less than the base case while those with the 1.0 m thickness were all about 90% less. These percentages correlate well with the sediment thickness differences from the base case that the two thickness cases represent. It may be possible to scale the arrival times of existing results of non-decaying contaminants by using a simple scaling factor based on changes in the unsaturated zone thickness.

The magnitude of the predicted groundwater concentration of radiological contaminants is affected by the value of the unsaturated zone thickness but not linearly. Decay of the contaminant is a function of time and the amount of time the contaminant spends in the unsaturated zone is proportional to the depth of the unsaturated zone. The arrival times of the peak concentration of radiological contaminants does appear to be affected in a manner similar to non-radiological contaminants.

The effect of changing the groundwater flow direction appears to have only a minimal effect on resulting groundwater concentrations, especially if the receptor wells are located the same distance from contamination sites for both flow directions. Reversing the site dimensions has little impact relative to the effect of changing the cumulative vadose zone sediment thickness.

Finally, the differences between GWMENU user-interface program and GWSCREEN version 2.4a discovered in this analysis appear to be insignificant relative to the large degree of uncertainty associated with most parameters involved in groundwater modeling.

REFERENCES

Anderson, S. R., D. J. Ackerman, and M. J. Liszewski, *Stratigraphic Data for Wells at and near the Idaho National Engineering Laboratory, Idaho*, U. S. Geological Survey Open-File Report 96-248, DOE/ID-22127, May 1996.

Rood, A. S., 1994, *GWSCREEN: A Semi Analytical Model for Assessment of the Groundwater Pathway from Surface and Buried Contamination: Version 2.0 Theory and Users Manual*, Idaho National Engineering Laboratory, EGG-GEO-10797, Revision 2, June 1994.

U.S. Department of Energy, *Comprehensive Well Survey for the Idaho National Engineering Laboratory: Revision 3*, DOE/ID-10402, 1994.